# Ultra small Angle Neutron Scattering from Amorphous Ni–Pd–P-Alloys

R. M. Hagenmayer, C. M. E. Zeyen[1], P. Lamparter, and S. Steeb

Max-Planck-Institut für Metallforschung, Institut für Werkstoffwissenschaft, Stuttgart, Germany
[1] Institut Laue Langevin, Grenoble, France

Z. Naturforsch. **49a**, 1203–1206 (1994); received October 26, 1993

Using a neutron double crystal spectrometer, thin amorphous Ni–Pd–P-samples were investigated at very small $Q$-values ($10^{-5}$ Å$^{-1} \leqq Q \leqq 10^{-3}$ Å$^{-1}$). The immersion method shows that the small angle scattering effect is mainly caused by surface scattering.

## 1. Introduction

The medium range structure of amorphous $Ni_{32}Pd_{52}P_{16}$ was investigated in [1], using small angle neutron scattering (SANS) down to $Q$-values of $10^{-3}$ Å$^{-1}$, where $Q$ is the modulus of the momentum transfer ($Q = 4\pi(\sin\Theta)/\lambda$; $2\Theta$ = scattering angle; $\lambda$ = neutron wavelength).

At ILL, Grenoble, the double crystal spectrometer S21 can be used as a Bonse-Hart camera down to $Q \cong 10^{-5}$ Å$^{-1}$, and it seemed interesting to study SANS of metallic glasses down to this very small $Q$-value. This means that the detectable size dimensions can reach $10^5$ Å. In the present work we investigated the amorphous alloys $Ni_{32}Pd_{52}P_{16}$ and $Ni_{20}Pd_{60}P_{20}$.

To study the influence of surface scattering on the total scattered intensity, the immersion technique [2, 3] was applied to the amorphous $Ni_{20}Pd_{60}P_{20}$ sample.

## 2. Experimental

### 2.1 Double Crystal Spectrometer

The double crystal spectrometer S21 is installed at the thermal H25 guide tube of the ILL-high flux reactor, Grenoble. The Bonse-Hart arrangement (Fig. 1) consists of a silicon crystal with the (331) planes parallel to its surface ($d_{331} = 1.2459$ Å). Neutrons with the wavelength 1.76 Å are reflected at a scattering angle $2\Theta_B = 90°$ and traverse the specimen. The transmitted beam is analyzed in a channel-cut crystal yielding threefold reflexion. Its reflecting surfaces $A_1$ and $A_2$ are also cut along the (331)-planes. By the multiple reflexion in the analyzer the intensity in the wings of the reflexion peaks, which can interfere with USANS, is reduced. Such crystals were first applied for X-ray small angle scattering [4]. Their application for neutrons is described in [5, 6].

The analyzing crystal is rotated by a motor in steps of 0.258 seconds of arc, which means for $\lambda = 1.76$ Å a $\Delta Q$ of $9 \cdot 10^{-6}$ Å$^{-1}$. A sample changer was used to measure for each $Q$-value the beam diffracted from the container with and without sample. For the immersion technique with amorphous $Ni_{20}Pd_{60}P_{20}$, first the intensity from the container filled with specimen and immersion liquid, and then the container filled with the immersion liquid only was measured. The containers were made from quartz. For details see [7].

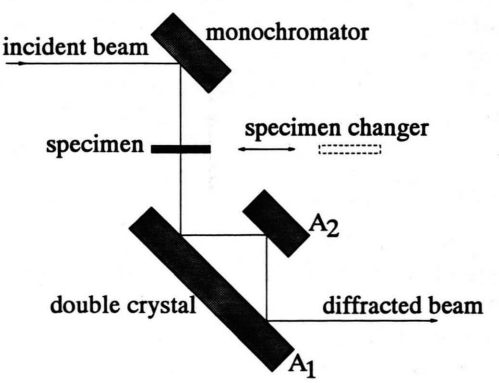


Fig. 1. Principle of the double crystal spectrometer.

Reprint requests to Prof. Dr. S. Steeb, Max-Planck-Institut für Metallforschung, Institut für Werkstoffwissenschaft, Seestraße 92, D-70174 Stuttgart.

0932-0784 / 93 / 1200-1203 $ 01.30/0. – Please order a reprint rather than making your own copy.

### *2.2 Evaluation*

The specimen is either mounted on a holder or in a container with immersion liquid. Arranging the specimen (S) within the specimen holder in the incident beam before the monochromator yields in the diffracted beam at $Q = 0$ the intensity $I_{S,O}$. Arranging the empty specimen holder $H$ or the container with immersion liquid but without specimen, respectively, at the same position yields the intensity $I_{H,O}$. The attenuation correction factor $G$ of the specimen then follows from

$$I_{S,O} = G \cdot I_{H,O}. \tag{1}$$

Of course, the $G$-factor must be determined from specimen to specimen. The small angle signal $K(Q)$ then is obtained as

$$K(Q) = \frac{1}{G} \cdot I_S(Q) - I_H(Q) \tag{2}$$

with

$I_S(Q)$ = intensity from specimen plus holder (or container with immersion liquid) in specimen position,

$I_H(Q)$ = intensity from holder (or container with immersion liquid) alone in specimen position.

### *2.3 Immersion Technique*

In [2] the so-called immersion technique was proposed. It allows to separate the effects of surface and volume scattering. A specimen container with smooth inner surface contains an immersion liquid which surrounds the specimen. If the immersion liquid has the same scattering length density $\eta$ as the specimen, surface scattering effects are eliminated and only volume scattering remains visible. Of course, the immersion liquid must totally wet the specimen surface. Mixtures of deuterated and natural ethyl alcohol (e.a.) can be adjusted to scattering length densities within the range $-0.35 \cdot 10^{10} \frac{\text{cm}}{\text{cm}^3} \leqq \eta \leqq +6.22 \cdot 10^{10} \frac{\text{cm}}{\text{cm}^3}$ corresponding to $0\ \text{vol.\%} \leqq v_{\text{deut.e.a.}} \leqq 100\ \text{vol.\%}$. This follows from the scattering lengths $b_H = -0.37 \cdot 10^{-12}$ cm and $b_D = +0.67 \cdot 10^{-12}$ cm.

The scattering lengths $b$ and mean atomic number densities $\varrho_0$ for $C_2H_5OH$, $C_2D_5OD$ as well as amorphous $Ni_{20}Pd_{60}P_{20}$ are compiled in Table 1.

It should be noted that the complete suppression of the surface effect is only possible for the simple case of a rough surface. Then the scattering intensity scales with the square of the difference $\Delta\eta$ of the scattering length densities of the specimen and of the immersion liquid. For the case of concentration fluctuations at the surface, such as precipitates, the surface scattering can only be reduced.

Table 1. Scattering length densities. $b$ = mean scattering length, $\eta = b \cdot \varrho_0$.

| | $b$ $[10^{-12}\ \text{cm}]$ | $\varrho_0$ $[10^{22}\ \text{cm}^{-3}]$ | $\eta$ $\left[10^{10}\ \frac{\text{cm}}{\text{cm}^3}\right]$ |
|---|---|---|---|
| $Ni_{20}Pd_{60}P_{20}$ | 0.6632 | 6.5 | 4.32 |
| $C_2H_5OH$ | −0.0372 | 9.294 | −0.346 |
| $C_2D_5OD$ | 0.6572 | 9.465 | 6.220 |

## 3. Results and Discussion

Amorphous Ni–Pd–P-alloys with phosphorous contents between 15 and 25 atom% can be produced by melt-spinning [1]. They show rather large thermodynamical (DSC) effects during relaxation. Those effects were ascribed to segregation of the glass-phase into two glass-phases [8, 9], however, also to formation of microcrystallites within an amorphous matrix [10]. Wide angle X-ray scattering experiments showed rather large structural changes during the relaxation process [11]. In the present study melt-spun specimens were used, namely amorphous $Ni_{32}Pd_{52}P_{16}$ 7 mm wide and amorphous $Ni_{20}Pd_{60}P_{20}$ 14 mm wide.

### *3.1 Specimens in Air*

Figure 2, upper curve, shows the $\log K(Q) - \log Q$-plot as obtained with the double crystal spectrometer with amorphous $Ni_{32}Pd_{52}P_{16}$. A linear behaviour is observed with gradient −1.8. In [1] also a linear behaviour was found with the same alloy in the region $-3 \leqq \log Q \leqq -1.7$. The gradient in that case amounted to −3.85.

It is not possible to draw a final conclusion from a quantitative comparison of both gradients because of the effects of smearing the SANS due to the linear collimation of the S21 instrument, whereas the point collimation instrument D11 at ILL used in [1] does not involve substantial smearing effects. It is expected that a desmearing procedure of the S21 data would result in a change of the gradient to a larger value,

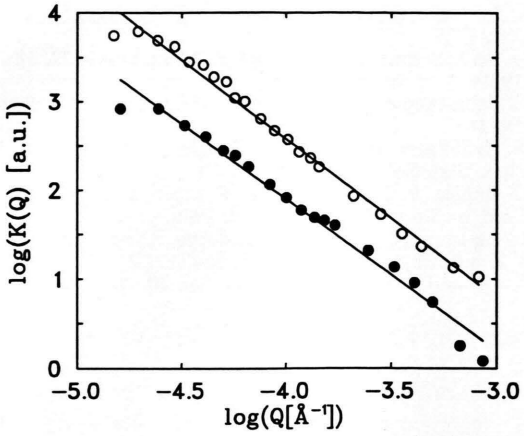


Fig. 2. SANS; double logarithmic plot of the intensity. (o) Amorphous $Ni_{32}Pd_{52}P_{16}$ in air. (•) Amorphous $Ni_{20}Pd_{60}P_{20}$ in 50 vol.% $C_2D_5OD$ and 50 vol.% $C_2H_5OH$; (—) fit with straight line.

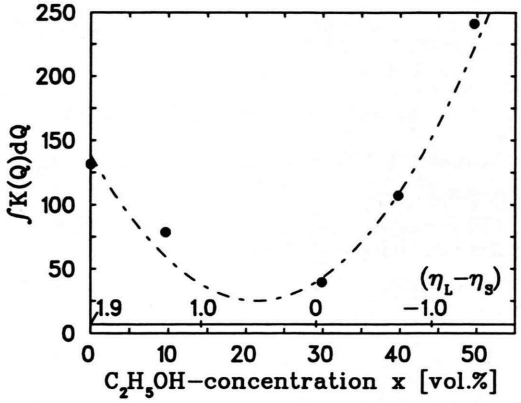


Fig. 3. Amorphous $Ni_{20}Pd_{60}P_{20}$; total intensity versus concentration $x$ of ethyl alcohol. $\eta_L - \eta_S$ is the scattering length density difference between liquid and sample (in units of $10^{10}$ cm$^{-2}$).

where the maximum change can be from $-1.8$ to $-2.8$. In [12] a desmearing procedure applied to an S21 SANS curve caused a change of a slope by one. Thus it is suggested that the gradient of the SANS of $Ni_{32}Pd_{52}P_{16}$ in a log-log representation is less steep in the range of very small $Q < 10^{-3}$ Å$^{-1}$ than in the range $Q > 10^{-3}$ Å$^{-1}$.

### *3.2 Immersion Technique with Amorphous $Ni_{20}Pd_{60}P_{20}$*

The sample changer was loaded with two containers. One was a container filled with the immersion liquid. The other contained within the immersion liquid twenty amorphous sample ribbons, each 15 μm thick. Thus a total thickness of about 0.3 mm was achieved.

Figure 2, lower curve, shows as an example $\log K(Q)$ versus $\log Q$ for amorphous $Ni_{20}Pd_{60}P_{20}$ within an immersion liquid containing 50 vol.% $C_2H_5OH$. The curves obtained with 0, 10, and 40 vol.%, respectively, differed strongly in their level but showed gradients similar to those presented in Figure 2. The scattering curve of the $Ni_{20}Pd_{60}P_{20}$ specimen inside the 30 vol.% $C_2H_5OH$-liquid showed within the limits given by the experimental accuracy only background scattering.

The effect of the immersion technique on the SANS signal is shown in Figure 3 as total intensity, integrated over the entire $Q$-range, versus the volume fraction $x$ of $C_2H_5OH$. We observe a strong influence of the alcohol mixture on the SANS, which proves the existence of surface scattering. In this case the SANS intensity is expected to scale with the square of the difference between the scattering length density of the sample $\eta_S$ and of the liquid $\eta_L$, respectively, which in turn is related linearly to the volume fraction $x$. The parabola in Fig. 3 was fitted to the experimental points. The minimum of this parabola lies at $x = 21.4$ vol.%. According to the figures in Table 1, $\eta_L - \eta_S = 0$ yields $x = 29.0$ vol.% as the expected point of the minimum. This shift of the minimum indicates a different composition of the sample at its surface compared with the bulk, indicating a lower Ni-concentration at the surface. In this respect an investigation on amorphous Fe–Ni–P–B [13] should be mentioned, where *P*-enrichment at the surface has also been found.

From the present results obtained with the immersion technique we deduce a strong influence of surface scattering during SANS-work with amorphous $Ni_{20}Pd_{60}P_{20}$ down to $Q$-values of $10^{-5}$ Å$^{-1}$. This means that for this amorphous alloy and most probably also for the amorphous $Ni_{32}Pd_{52}P_{16}$-alloy reported in the present work and in [1] a very strong surface scattering effect is superposed on a rather small share of bulk scattering.

*Acknowledgement*

Thanks are due to the ILL, Grenoble, for the allocation of beam time. Special thanks are due to R. Chagnon, P. Ledebt, and P. Lindner.

[1] M. Schaal, P. Lamparter, and S. Steeb, Z. Naturforsch. **44a,** 4 (1989).
[2] B. Rodmacq, Ph. Mangin, and A. Chamberod, J. de Physique **46,** C8-499 (1985).
[3] M. Maret, P. Chieux, and P. Hicter, Z. Phys. Chemie **157,** 109 (1988).
[4] U. Bonse, M. Hart, Zeitschrift für Physik **189,** 151 (1965).
[5] D. Schwahn, A. Miksovsky, H. Rauch, E. Seidl, G. Zugarek, Nucl. Instrum. and Meth. in Physics Research **A 239,** 229 (1985).
[6] A. Miksovsky, diploma thesis, Atominstitut der Österreichischen Universität, Wien 1983.
[7] R. M. Hagenmayer, diploma thesis, University of Stuttgart, 1989.
[8] G. Schluckebier and B. Predel, Z. Metallkunde **72,** 181 (1981).
[9] G. Schluckebier and B. Predel, Z. Metallkunde **74,** 569 (1983).
[10] N. Willmann, W. Mader, E. Wachtel, and B. Predel, Phys. Stat. Sol. (a) **104,** 369 (1987).
[11] E. Bühler, P. Lamparter, and S. Steeb, Proc. 6th Int. Conf. on Liqu. and Amor. Met. **1986,** p. 91.
[12] P. Leisieur, P. Lindner, C. Desforge, J. Lambard, and T. Zemb, Physica **B 180 & 181,** 564 (1992).
[13] Z. Qu and K. H. Kuo, J. Mater. Sci. **20,** 2023 (1985).